# Vapour-liquid equilibria of the CH 4 + CO 2 + H 2 S ternary system with two different global compositions: experiments and modelling

Pascal Théveneau, Xiaochun Xu, Olivier Baudouin, Jean-Noël Jaubert, Paola Ceragioli, Christophe Coquelet

# Vapour-liquid equilibria of the $CH_4$ + $CO_2$ + $H_2S$ ternary system with two different global compositions: experiments and modelling

Pascal Theveneau[1], Xiaochun Xu[2], Olivier Baudouin[3], Jean-Noël Jaubert[2], Paola Ceragioli[4], Christophe Coquelet[1*]

[1]MINES ParisTech, PSL Université, CTP- Centre Thermodynamique des Procédés, 35 rue Saint Honoré, 77300 Fontainebleau France

[2]Université de Lorraine, École Nationale Supérieure des Industries Chimiques, Laboratoire Réactions et Génie des Procédés (UMR CNRS 7274), 1 rue Grandville, 54000, Nancy, France

[3]ProSim SA, Immeuble Stratège A, 51 rue Ampère, 31670 Labège, France

[4]Eni UPS, Via Maritano 26, 20097 San Donato Milanese, Milano, Italy

**Abstract**

The vapor-liquid equilibrium for two mixtures containing methane, carbon dioxide and hydrogen sulphide was determined experimentally by a static-analytic method. Thirty-one data points were acquired for a range of temperatures from 243 K to 333 K at pressures up to 11 MPa. The measured data were correlated with the Peng Robinson equation of state (EoS) and different mixing rules, which led to the conclusion that a cubic EoS could simultaneously predict the existence of a 3-phase region and 2 critical points on the constant-composition two-phase boundary curve.

**Key words:** Equation of state, Static-analytic method, data treatment, gas processing

(*) author to whom correspondence should be addressed

E-mail: christophe.coquelet@mines-paristech.fr

Tel: +33 164694968 Fax: +33 164694968

## Introduction

In the context of energetic transition, it appears that natural gas could be the best replacement for oil or coal. Natural gas is usually composed of methane and other hydrocarbons, but in recent decades, a number of sour natural gas sources and gas-condensate fields have been discovered around the world. Some of them contain large amounts of sulphur compounds, such as hydrogen sulphide, together with carbon dioxide[1]. Therefore, the oil and gas industry requires vapour-liquid equilibrium data for mixtures containing methane + hydrogen sulphide + carbon dioxide to develop accurate models for calculating the thermodynamic properties of these complex natural gases. The expected final result is an equation of state (EoS) that could be used to determine the phase diagram, the compressibility and the density of sour natural gases within large temperature and pressure ranges.

To obtain accurate results with an EoS, the molecular interactions between the different components of a mixture must be characterized. Such characterization is usually performed through the definition of the mixing and combining rules[2] for the parameters of the EoS. The combining rules typically require the determination of the binary interaction parameters (BIPs), which can be either fitted based on experimental data or estimated by group-contribution methods such as those used in the PPR78[3,4], PR2SRK[5] and PSRK[6] predictive thermodynamic models.

The ternary system $CH_4$ + $CO_2$ + $H_2S$ is composed of 3 binary systems that must be analysed. Many experimental data are available for the binary system $CH_4$ + $CO_2$[7–19] which can be classified as a type I system according to the classification scheme of van Konynenburg and Scott[20,21]. Due to the value of the melting temperature of $CO_2$, a solid-liquid-vapor equilibrium may appear at temperatures higher than the critical temperature of $CH_4$[22]. The binary system $CO_2$ + $H_2S$, which is also a type I system, was studied in our research laboratory (CTP) in 2013. The vapour–liquid equilibrium data we measured were published in Chapoy et al.[23] and were found to be in good agreement with existing data in the literature about the same binary system. The last binary system, $CH_4$ + $H_2S$, was also previously studied by our research group (in 2014) because it is a key system for the development of the SPREX $H_2S$ process[24]. It can be classified as a type III system according to the classification scheme of van Konynenburg and Scott, meaning that at low temperature, the system exhibits vapour-liquid-liquid equilibria. Due to its complexity, such a system was used as an example by Heidemann and Khalil[25] to describe the computation of the mixture critical line for type III systems. In 1999, Bluma and Deiters[26] proposed a classification scheme for phase diagrams of ternary fluid systems. As previously stated, the studied ternary system ($CH_4$ + $CO_2$ + $H_2S$) contains one type III binary subsystem and two type I binary subsystems. According to Bluma and Deiters, such a configuration corresponds to a type III ternary system (denoted T-III). Moreover, phase equilibria measurements were performed with such a ternary system by Ng et al.[27,28] who

highlighted the existence of a vapour-liquid-liquid equilibrium region and confirmed the type of the ternary system.

In this paper, new vapour-liquid equilibrium data are presented for two different global compositions of the ternary system. The experimental method used in this work is a static-analytic type method. This method takes advantage of a capillary sampler (ROLSI®, Armines' patent) developed in the CTP laboratory. Table 1 presents the composition of the 2 studied mixtures, which were purchased from Air Products, along with the corresponding uncertainties. These 2 mixtures were also analysed by gas chromatography in the CTP laboratory, and the results of this analysis can be found in Table 1.

[Table 1]

The measured data were correlated with the Peng-Robinson[29,30] (PR) equation of state (EoS) combined with the Wong-Sandler mixing rules[31]. The cubic EoS was used without volume translation[32–34] because this work focuses only on fluid phase equilibria calculations. Meanwhile, the PPR78[3,35] model was applied for predicting the vapor-liquid equilibrium (VLE) and phase boundaries of the ternary system.

**Experimental section**

The measurements were performed with an apparatus based on the static-analytic method using an equilibrium cell fitted with a movable electromagnetic ROLSI® sampler. This apparatus is similar to the one used by Théveneau et al.[36]. It was thermoregulated by means of a liquid bath. The temperature stability of the liquid bath containing the equilibrium cell was within +/- 0.02 °C. The cell (with a total volume of approximately 4 $cm^3$) consisted of a sapphire tube that was pressed between two titanium flanges. Sealing was achieved by using polymer O-rings. The bottom of the cell held one platinum probe and the stirring assembly. The top of the cell held one platinum probe and the capillary of the movable ROLSI ® electromagnetic sampler, which was connected to a gas chromatograph (GC) for liquid and vapour sample analyses, as well as two loading valves. For both mixtures, the transfer line and the mixture container were heated to avoid partial condensation during transfer. The calibration of the pressure transducer (8 MPa, Druck PTX 611 type) connected to the equilibrium cell was performed with a dead-weight tester (Desgranges and Huot type 5202 S CP, 2-40 MPa range). The atmospheric pressure was measured with a Resonant Sensor Barometer (Druck, model DPI 141). The accuracy of the pressure measurement was estimated to be within +/- 0.0025 MPa. The two 100 Ω platinum probes, which were placed inside holes drilled in the top and bottom flanges of the cell, as well as the probe connected to the mixture container were calibrated with a 25 Ω reference platinum probe (Tinsley type 5187) connected to a micro-ohmmeter (Hewlett

Packard 34420A). The reference probe was calibrated by LNE (Paris) according to the ITS 90 scale. The accuracy of the temperature measurement was estimated to be within +/- 0.025 °C. GC analyses were performed using a gas chromatograph (Varian, model 3800) fitted with a thermal conductivity detector (TCD). The analytical column was a Porapack Q packed column (2 metres in length, 1/8" wide, 100/120 mesh) thermostated at 40 °C in the GC oven. Known volumes of pure methane, carbon dioxide and hydrogen sulphide were directly injected into the injector of the gas chromatograph by using calibrated airtight syringes of various volumes. Calibration curves showing the "component peak area versus the component mole number" appeared to be linear within the experimental uncertainties. The mean relative accuracy of the measurement of the experimental mole number was estimated to be within +/- 2 % for $CH_4$, +/- 1.5 % for $CO_2$ and +/- 2 % for $H_2S$. When the pressure and temperature were constant in the cell, each phase was analysed by gas chromatography using the movable electromagnetic ROLSI® sampler. Generally, no more than three samplings were necessary to purge the capillary and to obtain representative samples of the mixture at equilibrium. Approximately five to ten samples were obtained from each phase for composition determination. As highlighted by Eq. (1), the uncertainty in the composition can be calculated based on the knowledge of the uncertainty of each mole number:

$$u(x_i) = \sqrt{\sum_{i}^{ncomp} \left( \frac{\partial x_i}{\partial n_i} \right)^2_{i \neq j} u^2(n_i)} \qquad (1)$$

For a binary system, one obtains:

$$u(x_1) = x_1(1 - x_1) \sqrt{\left( \frac{u(n_1)}{n_1} \right)^2 + \left( \frac{u(n_2)}{n_2} \right)^2} \qquad (2)$$

For a ternary system, one obtains:

$$u(x_1) = x_1 \sqrt{(1 - x_1)^2 \left( \frac{u(n_1)}{n_1} \right)^2 + x_2^2 \left( \frac{u(n_2)}{n_2} \right)^2 + x_3^2 \left( \frac{u(n_3)}{n_3} \right)^2} \qquad (3)$$

The maximum uncertainty in the mole fraction was found to be u(z)=0.007.

**Experimental results**

Tables 2 and 3 present the measured vapour-liquid equilibrium data for mixtures 1 and 2, respectively. The global composition of each mixture can be found in Table 1.

[Table 2]

[Table 3]

**Data treatment**

All the experimental data were correlated with Simulis Thermodynamics software, which was developed by ProSim SA. The Peng Robinson EoS with different mixing rules was chosen because of its simplicity and its widespread utilization in chemical engineering. Its formulation is:

$$p = \frac{RT}{v-b} - \frac{a_c \cdot \alpha(T)}{v(v+b)+b(v-b)} \quad (4)$$

The critical temperature ($T_c$) and critical pressure ($p_c$) used for estimating $b$ and $a_c$ are given in Table 4 for each pure compound. The acentric factor (ω) used in the PPR78 model is also reported. In this paper, two different mixing rules were successively used to correlate the experimental data measured in this study. In the first analysis, the Wong-Sandler (WS) mixing rules were used, and in the second analysis, classical van der Waals mixing rules combined with a group contribution method to estimate the BIPS (the so-called PPR78 model) were used.

*Correlation of the measured data with the PR EoS and WS mixing rules.*

In this paper, to accurately predict the vapor pressures of each component, the WS mixing rules are used in conjunction with a specific alpha function, namely, the Mathias-Copeman alpha function[37]. This function, given below, was developed especially for polar compounds and has three adjustable parameters. Although it is non-consistent[38–40], its accuracy has been demonstrated.

If $T<T_c$, $$\alpha(T) = \left[1 + c_1\left(1-\sqrt{\frac{T}{T_C}}\right) + c_2\left(1-\sqrt{\frac{T}{T_C}}\right)^2 + c_3\left(1-\sqrt{\frac{T}{T_C}}\right)^3\right]^2 \quad (5)$$

If $T>T_c$, $$\alpha(T) = \left[1 + c_1\left(1-\sqrt{\frac{T}{T_C}}\right)\right]^2 \quad (6)$$

The component-dependent $c_1$, $c_2$ and $c_3$ parameters are given in Table 4. They originate from Reid et al.[41]

[Table 4]

The WS mixing rules[31] are written as follows:

$$\begin{cases} b(T,\mathbf{x}) = \dfrac{\displaystyle\sum_{i=1}^{p}\sum_{j=1}^{p} x_i x_j \dfrac{\left(b_i - \dfrac{a_i}{RT}\right)+\left(b_j - \dfrac{a_j}{RT}\right)}{2}(1-k_{ij})}{1+\dfrac{\mathcal{G}^E}{RTC_{EoS}} - \displaystyle\sum_{i=1}^{p} x_i \dfrac{a_i(T)}{RTb_i}} \\ a(T,\mathbf{x}) = b(\mathbf{x})\left[\displaystyle\sum_{i=1}^{p} x_i \dfrac{a_i(T)}{b_i} - \dfrac{\mathcal{G}^E}{C_{EoS}}\right] \\ \text{For the PR EoS}: C_{EoS} = \dfrac{\sqrt{2}}{2}\ln\left(1+\sqrt{2}\right) \approx 0.6232 \end{cases} \quad (7)$$

$k_{ij}$ is a temperature-independent binary interaction parameter, and the activity coefficient model ( $\mathcal{G}^E$ ) may be chosen from among the classical forms of the molar excess Gibbs energy functions (such as the Redlich-Kister, Margules, Wilson, Van Laar, NRTL, UNIQUAC, and UNIFAC functions). In this study, it was decided to use the 3-parameter NRTL[42] model:

$$\frac{g^E(T,P,x_i)}{RT} = \sum_i x_i \sum_j \frac{x_j \exp\left(-\alpha_{ji}\dfrac{\tau_{ji}}{RT}\right)}{\displaystyle\sum_k x_k \exp\left(-\alpha_{ki}\frac{\tau_{ki}}{RT}\right)}\tau_{ji} \quad (8)$$

$\tau_{ii} = 0$ and $\alpha_{ii} = 0$. $\alpha_{ji}$, $\tau_{ji}$ and $\tau_{ij}$ are the adjustable parameters. In this study, the classical value $\alpha_{ji} = 0.3$ was selected. $\tau_{ji}$ and $\tau_{ij,}$, which are considered temperature-independent, were adjusted directly on the experimental VLE data with a modified Simplex[43] algorithm by minimizing the following objective function:

$$\mathrm{F} = \frac{100}{\mathrm{N}}\left[\sum_1^{\mathrm{N}}\left(\frac{\mathrm{p_{exp}} - \mathrm{p_{cal}}}{\mathrm{p_{exp}}}\right)^2 + \sum_1^{\mathrm{N}}\left(\frac{\mathrm{y_{exp}} - \mathrm{y_{cal}}}{\mathrm{y_{exp}}}\right)^2\right] \quad (9)$$

where $N$ is the number of data points, $p_{exp}$ is the experimental pressure, $p_{cal}$ is the calculated pressure, and $y_{exp}$ and $y_{cal}$ are the experimental and calculated vapour phase molar fractions, respectively. The results are presented in Table 5, and the deviations in Figure 1 reveal that all the experimental data points are accurately correlated by the model. The parameters are presented in Table 6.

[Table 5]

[Figure 1]

[Table 6a]

[Table 6b]

*Accuracy of the WS mixing rules used to correlate other literature data.*

In 1985, Ng et al.[27,28] published some data on the same ternary system examined in this study with different global composition ($CH_4$: 0.4988, $CO_2$: 0.0987, $H_2S$: 0.4022). Using the PR EoS combined with the WS mixing rules and the parameters that were adjusted based on the data measured in this paper, a bubble-point algorithm was used to predict the data obtained by Ng et al. The deviations are shown in Table 7 and Figure 2. They are dispersed, but on average, the data were accurately predicted within the temperature range in which the parameters were fitted. Outside of the temperature range in which our data were acquired, the deviations are higher.

[Table 7]

[Figure 2]

*Correlation of the measured data and other literature data with the PPR78 model*

In this section, the application of the PPR78 model[3,44,45] to predict the VLE properties and the phase behaviour of the $CH_4$-$CO_2$-$H_2S$ system is discussed. Such a model combines the well-established PR-EoS (with the Soave[46] alpha function) and a group-contribution method to estimate the temperature-dependent binary interaction parameters, $k_{ij}^{PR}(T)$, which appear in the equations derived from the classical Van der Waals one−fluid mixing rules:

$$\begin{cases} a = \sum_{i=1}^{N}\sum_{j=1}^{N} x_i x_j \sqrt{a_i(T)\times a_j(T)}\left[1-k_{ij}^{PR}(T)\right] \\ b = \sum_{i=1}^{N} x_i b_i \end{cases} \quad (10)$$

and,

$$k_{ij}^{PR}(T) = \frac{-\frac{1}{2}\left[\sum_{k=1}^{N_g}\sum_{l=1}^{N_g}(\alpha_{ik}-\alpha_{jk})(\alpha_{il}-\alpha_{jl})A_{kl}\cdot\left(\frac{298.15}{T/K}\right)^{\left(\frac{B_{kl}}{A_{kl}}-1\right)}\right]-\left(\frac{\sqrt{a_i(T)}}{b_i}-\frac{\sqrt{a_j(T)}}{b_j}\right)^2}{2\frac{\sqrt{a_i(T)\cdot a_j(T)}}{b_i\cdot b_j}} \quad (11)$$

The $N_g$ variable represents the number of different groups defined according to the group-contribution method. The $\alpha_{ik}$ variable represents the fraction of molecule *i* occupied by group *k* (occurrence of group *k* in molecule *i* divided by the total number of groups present in molecule *i*).

The group-interaction parameters $A_{kl} = A_{lk}$ and $B_{kl} = B_{lk}$ (where $k$ and $l$ are two different groups) were determined during the development of the model. Those parameters that are needed to perform the calculations for the ternary system $CH_4/CO_2/H_2S$ are shown in Table 8.

[Table 8]

The deviations between the experimental VLE data and the predictions of the PPR78 model for both the data measured in this study and those measured by Ng et al.[27,28] are shown in Figure 3 and Figure 4, respectively. As shown in these figures, the deviations were satisfactory (<10 %) for most cases. However, the deviations may become very high, especially when the slope of the bubble curve becomes very steep at low temperatures (a small change in temperature greatly changes the bubble pressure).

[Figure 3]

[Figure 4]

*Prediction of the (P,T) envelopes with the PR EoS and different mixing rules*

Meanwhile, the PPR78 model and the PR EoS combined with the WS mixing rules were applied to predicting the PT envelopes of the ternary $CH_4$-$CO_2$-$H_2S$ mixture with different fixed global compositions. It was decided to perform the calculations according to the two global compositions studied in this paper and the global composition reported by Ng et al.[27] As explained by the authors, this ternary system (with the composition they studied) exhibits a very narrow three-phase region at lower temperatures. The two-phase boundary curve commences at a dew point locus that passes through an upper retrograde region and terminates at a vapour-liquid critical point. The phase boundary then follows a bubble point locus that terminates at a liquid-liquid critical point. After this, the boundary turns sharply upward at higher pressures and lower temperatures and separates the single phase from the liquid-liquid region. As shown in Figure 5, the PPR78 model can reproduce these complex phase behaviours for the mixture and accurately predict the three-phase equilibrium region. As previously discussed, the $CH_4$-$CO_2$ mixture and the $CO_2$-$H_2S$ mixture belong to the type I system, whereas the $CH_4$-$H_2S$ mixture is a type III system according to the classification scheme of Van Konynenburg and Scott. As discussed in the literature[47], cubic equations of state based on van der Waals-type mixing rules with only one binary interaction parameter present difficulties for modelling the critical loci of type III systems. Indeed, at least two binary interaction parameters are needed for the modelling of these systems. It is thus not surprising to observe that the PPR78 model is not able to locate the two critical points at the right places on the boundary curve. The results obtained with the WS mixing rules are shown in Figure 6, which makes

it possible to conclude that the selected mixing rules accurately predict the cricondentherm and cricondenbar but do not predict the existence of the two critical points.

The phase boundaries of two mixtures reported in this work that were predicted with the PPR78 model and the PR EoS with the WS mixing rules are presented in Figures 7 and 8, respectively. For mixture 1, a classical PT envelope that included a dew-point curve and a bubble-point curve was obtained, and the 2 models showed very comparable results (see Figures 7a and 7b). For mixture 2, a PT envelope similar to the one reported by Ng et al. was obtained. However, for the global composition, the PPR78 model was unable to predict the existence of the bubble curve and consequently the existence of the 2 critical points. However, the PR EoS with the WS mixing rules predicted the correct topology of the phase envelope.

[Figure 5]

[Figure 6]

[Figure 7]

[Figure 8]

**Conclusion**

New experimental vapor-liquid equilibrium data were acquired for the ternary $CH_4$ + $CO_2$ + $H_2S$ system at temperatures between 243 and 333 K (U(T)=0.03 K) and at pressures up to 11 MPa (U(p)=0.003 MPa) with a $U_{max}(z)$=0.007. With the aid of the software Simulis Thermodynamics, the data could be accurately correlated with the Peng Robinson EoS combined with the Wong Sandler mixing rules and the NRTL activity coefficient model. Such a thermodynamic model was also used to correlate the data published by Ng et al., and the deviations were found to be acceptable within the range of temperatures in which the parameters were fitted, i.e., within the temperature range in which the experiments were performed.

The predictive PPR78 model, which is available in Simulis Thermodynamics, was also used to predict the same data. The resulting deviations were satisfactory in most cases but were very high when the slope of the bubble curve was very steep at low temperatures.

In the end, both models were used to predict the PT envelopes of the ternary $CH_4$-$CO_2$-$H_2S$ mixture with different fixed global compositions. Both models succeeded in predicting the existence of a 3-phase region and the 2 critical points.

**Acknowledgements**

Ing. Pascal Théveneau and Professor Christophe Coquelet would like to thank Professor Dominique Richon for fruitful discussions.

**References**

(1) Hajiw, M. Hydrate Mitigation in Sour and Acid Gases, Mines ParisTech, 2014.
(2) Sandler, S. I.; Orbey, H. Mixing and Combining Rules. In *Equations of state for fluids and fluid mixtures. Part I.*; Experimental thermodynamics; Elsevier: Amsterdam ; New York, 2000; pp 321–358.
(3) Jaubert, J.-N.; Mutelet, F. VLE Predictions with the Peng-Robinson Equation of State and Temperature-Dependent $k_{ij}$ Calculated through a Group Contribution Method. *Fluid Phase Equilibria* **2004**, *224* (2), 285–304.
(4) Xu, X.; Jaubert, J.-N.; Privat, R.; Arpentinier, P. Prediction of Thermodynamic Properties of Alkyne-Containing Mixtures with the *E*-PPR78 Model. *Ind. Eng. Chem. Res.* **2017**, *56* (28), 8143–8157.
(5) Jaubert, J.-N.; Privat, R. Relationship between the Binary Interaction Parameters ($k_{ij}$) of the Peng–Robinson and Those of the Soave–Redlich–Kwong Equations of State: Application to the Definition of the PR2SRK Model. *Fluid Phase Equilibria* **2010**, *295* (1), 26–37.
(6) Holderbaum, T.; Gmehling, J. PSRK: A Group Contribution Equation of State Based on UNIFAC. *Fluid Phase Equilibria* **1991**, *70* (2–3), 251–265.
(7) Bian, B.; Wang, Y.; Shi, J.; Zhao, E.; Lu, B. C.-Y. Simultaneous Determination of Vapor-Liquid Equilibrium and Molar Volumes for Coexisting Phases up to the Critical Temperature with a Static Method. *Fluid Phase Equilibria* **1993**, *90* (1), 177–187.
(8) Al-Sahhaf, T. A.; Kidnay, A. J.; Sloan, E. D. Liquid + Vapor Equilibriums in the Nitrogen + Carbon Dioxide + Methane System. *Ind. Eng. Chem. Fundam.* **1983**, *22* (4), 372–380.
(9) Knapp, H.; Yang, X.; Zhang, Z. Vapor—Liquid Equilibria in Ternary Mixtures Containing Nitrogen, Methane, Ethane and Carbondioxide at Low Temperatures and High Pressures. *Fluid Phase Equilibria* **1990**, *54*, 1–18.
(10) Wei, M. S.-W.; Brown, T. S.; Kidnay, A. J.; Sloan, E. D. Vapor + Liquid Equilibria for the Ternary System Methane + Ethane + Carbon Dioxide at 230 K and Its Constituent Binaries at Temperatures from 207 to 270 K. *J. Chem. Eng. Data* **1995**, *40* (4), 726–731.
(11) Xu, N.; Dong, J.; Wang, Y.; Shi, J. High Pressure Vapor Liquid Equilibria at 293 K for Systems Containing Nitrogen, Methane and Carbon Dioxide. *Fluid Phase Equilibria* **1992**, *81*, 175–186.
(12) Arai, Y.; Kaminishi, G.-I.; Saito, S. The Experimental Determination Of The P-V-T-X Relations For The Carbon Dioxide-Nitrogen And The Carbon Dioxide-Methane Systems. *J. Chem. Eng. Jpn.* **1971**, *4* (2), 113–122.
(13) Davalos, J.; Anderson, W. R.; Phelps, R. E.; Kidnay, A. J. Liquid-Vapor Equilibria at 250.00K for Systems Containing Methane, Ethane, and Carbon Dioxide. *J. Chem. Eng. Data* **1976**, *21* (1), 81–84.
(14) Webster, L. A.; Kidnay, A. J. Vapor−Liquid Equilibria for the Methane−Propane−Carbon Dioxide Systems at 230 K and 270 K. *J. Chem. Eng. Data* **2001**, *46* (3), 759–764.
(15) Mraw, S. C.; Hwang, S.-C.; Kobayashi, R. Vapor-Liquid Equilibrium of the Methane-Carbon Dioxide System at Low Temperatures. *J. Chem. Eng. Data* **1978**, *23* (2), 135–139.
(16) Donnelly, H. G.; Katz, D. L. Phase Equilibria in the Carbon Dioxide–Methane System. *Ind. Eng. Chem.* **1954**, *46* (3), 511–517.
(17) Somait, F. A.; Kidnay, A. J. Liquid-Vapor Equilibriums at 270.00 K for Systems Containing Nitrogen, Methane, and Carbon Dioxide. *J. Chem. Eng. Data* **1978**, *23* (4), 301–305.
(18) Kaminishi, G.-I.; Arai, Y.; Saito, S.; Maeda, S. Vapor-Liquid Equilibria For Binary And Ternary Systems Containing Carbon Dioxide. *J. Chem. Eng. Jpn.* **1968**, *1* (2), 109–116.

(19) Neumann, A.; Walch, W. Dampf/Flüssigkeits-Gleichgewicht CO2/CH4 im Bereich tiefer Temperaturen und kleiner CO2-Molenbrüche. *Chem. Ing. Tech.* **1968**, *40* (5), 241–244.
(20) Van Konynenburg, P. H.; Scott, R. L. Critical Lines and Phase Equilibria in Binary Van Der Waals Mixtures. *Philos. Trans. R. Soc. Math. Phys. Eng. Sci.* **1980**, *298* (1442), 495–540.
(21) Privat, R.; Jaubert, J.-N. Classification of Global Fluid-Phase Equilibrium Behaviors in Binary Systems. *Chem. Eng. Res. Des.* **2013**, *91* (10), 1807–1839.
(22) Stringari, P.; Campestrini, M.; Coquelet, C.; Arpentinier, P. An Equation of State for Solid–Liquid–Vapor Equilibrium Applied to Gas Processing and Natural Gas Liquefaction. *Fluid Phase Equilibria* **2014**, *362*, 258–267.
(23) Chapoy, A.; Coquelet, C.; Liu, H.; Valtz, A.; Tohidi, B. Vapour–Liquid Equilibrium Data for the Hydrogen Sulphide (H2S)+carbon Dioxide (CO2) System at Temperatures from 258 to 313K. *Fluid Phase Equilibria* **2013**, *356*, 223–228.
(24) Coquelet, C.; Valtz, A.; Stringari, P.; Popovic, M.; Richon, D.; Mougin, P. Phase Equilibrium Data for the Hydrogen Sulphide+methane System at Temperatures from 186 to 313K and Pressures up to about 14MPa. *Fluid Phase Equilibria* **2014**, *383*, 94–99.
(25) Heidemann, R. A.; Khalil, A. M. The Calculation of Critical Points. *AIChE J.* **1980**, *26* (5), 769–779.
(26) Bluma, M.; Deiters, U. K. A Classification of Phase Diagrams of Ternary Fluid Systems. *Phys. Chem. Chem. Phys.* **1999**, *1* (18), 4307–4313.
(27) Ng, H.-J.; B. Robinson, D.; Leu, A.-D. Critical Phenomena in a Mixture of Methane, Carbon Dioxide and Hydrogen Sulfide. *Fluid Phase Equilibria* **1985**, *19* (3), 273–286.
(28) Robinson, D. B.; Ng, H.-J.; Leu, A. D. Behavior of $CH_4$-$CO_2$-$H_2S$ Mixtures at Sub-Ambient Temperatures (RR-47). *Res. Rep. GPA* **1981**, 1–38.
(29) Peng, D.-Y.; Robinson, D. B. A New Two-Constant Equation of State. *Ind. Eng. Chem. Fundam.* **1976**, *15* (1), 59–64.
(30) Pina-Martinez, A.; Privat, R.; Jaubert, J.-N.; Peng, D.-Y. Updated Versions of the Generalized Soave α-Function Suitable for the Redlich-Kwong and Peng-Robinson Equations of State. *Fluid Phase Equilibria* **2019**, *485*, 264–269.
(31) Wong, D. S. H.; Sandler, S. I. A Theoretically Correct Mixing Rule for Cubic Equations of State. *AIChE J.* **1992**, *38* (5), 671–680.
(32) Péneloux, A.; Rauzy, E.; Freze, R. A Consistent Correction for Redlich-Kwong-Soave Volumes. *Fluid Phase Equilibria* **1982**, *8* (1), 7–23.
(33) Jaubert, J.-N.; Privat, R.; Le Guennec, Y.; Coniglio, L. Note on the Properties Altered by Application of a Péneloux-Type Volume Translation to an Equation of State. *Fluid Phase Equilibria* **2016**, *419*, 88–95.
(34) Privat, R.; Jaubert, J.-N.; Le Guennec, Y. Incorporation of a Volume Translation in an Equation of State for Fluid Mixtures: Which Combining Rule? Which Effect on Properties of Mixing? *Fluid Phase Equilibria* **2016**, *427*, 414–420.
(35) Qian, J.-W.; Jaubert, J.-N.; Privat, R. Phase Equilibria in Hydrogen-Containing Binary Systems Modeled with the Peng-Robinson Equation of State and Temperature-Dependent Binary Interaction Parameters Calculated through a Group-Contribution Method. *J. Supercrit. Fluids* **2013**, *75*, 58–71.
(36) Théveneau, P.; Coquelet, C.; Richon, D. Vapour–Liquid Equilibrium Data for the Hydrogen Sulphide+n-Heptane System at Temperatures from 293.25 to 373.22 K and Pressures up to about 6.9 MPa. *Fluid Phase Equilibria* **2006**, *249* (1–2), 179–186.
(37) Mathias, P. M.; Copeman, T. W. Extension of the Peng-Robinson Equation of State to Complex Mixtures: Evaluation of the Various Forms of the Local Composition Concept. *Fluid Phase Equilibria* **1983**, *13*, 91–108.
(38) Le Guennec, Y.; Lasala, S.; Privat, R.; Jaubert, J.-N. A Consistency Test for α-Functions of Cubic Equations of State. *Fluid Phase Equilibria* **2016**, *427*, 513–538.
(39) Le Guennec, Y.; Privat, R.; Jaubert, J.-N. Development of the Translated-Consistent *tc*-PR and *tc*-RK Cubic Equations of State for a Safe and Accurate Prediction of Volumetric, Energetic

and Saturation Properties of Pure Compounds in the Sub- and Super-Critical Domains. *Fluid Phase Equilibria* **2016**, *429*, 301–312.
(40) Le Guennec, Y.; Privat, R.; Lasala, S.; Jaubert, J.-N. On the Imperative Need to Use a Consistent α-Function for the Prediction of Pure-Compound Supercritical Properties with a Cubic Equation of State. *Fluid Phase Equilibria* **2017**, *445*, 45–53.
(41) Reid, R. C.; Prausnitz, J. M.; Poling, B. E. *The Properties of Gases and Liquids*, 4th ed.; McGraw-Hill: New York, 1987.
(42) Renon, H.; Prausnitz, J. M. Local Compositions in Thermodynamic Excess Functions for Liquid Mixtures. *AIChE J.* **1968**, *14* (1), 135–144.
(43) Åberg, E. R.; Gustavsson, A. G. T. Design and Evaluation of Modified Simplex Methods. *Anal. Chim. Acta* **1982**, *144*, 39–53.
(44) Vitu, S.; Privat, R.; Jaubert, J.-N.; Mutelet, F. Predicting the Phase Equilibria of $CO_2$ + Hydrocarbon Systems with the PPR78 Model (PR EoS and $k_{ij}$ Calculated through a Group Contribution Method). *J. Supercrit. Fluids* **2008**, *45* (1), 1–26.
(45) Privat, R.; Mutelet, F.; Jaubert, J.-N. Addition of the Hydrogen Sulfide Group to the PPR78 Model (Predictive 1978, Peng-Robinson Equation of State with Temperature-Dependent $k_{ij}$ Calculated through a Group Contribution Method). *Ind. Eng. Chem. Res.* **2008**, *47* (24), 10041–10052.
(46) Soave, G. Equilibrium Constants from a Modified Redlich-Kwong Equation of State. *Chem. Eng. Sci.* **1972**, *27* (6), 1197–1203.
(47) Lasala, S.; Chiesa, P.; Privat, R.; Jaubert, J.-N. Modeling the Thermodynamics of Fluids Treated by $CO_2$ Capture Processes with Peng-Robinson + Residual Helmholtz Energy-Based Mixing Rules. *Ind. Eng. Chem. Res.* **2017**, *56* (8), 2259–2276.

**List of Tables**

**List of figures**

**Table 1.** Global composition of the 2 studied mixtures: Air Products certified composition (standard ISO 9001:2000) and CTP analysis.

| Chemical/CAS number | Formula | CTP analysis | | | Air Products certified values | | |
|---|---|---|---|---|---|---|---|
| | | Global composition (Mol%) | Uncertainty (Mol%, k=2) | Experimental method | Global composition (Mol%) | Uncertainty (Mol%, k=2) | Experimental method |
| | | | | | Mixture 1 | | |
| Methane/74-82-8 | $CH_4$ | 4.06 | 0.02 | Gas Chromatography | 4.106 | 0.68 | Gravimetric method |
| Carbon dioxide/124-38-9 | $CO_2$ | 3.11 | 0.03 | | 3.077 | 0.06 | |
| Hydrogen sulphide/7783-06-4 | $H_2S$ | 92.83 | 0.05 | | 92.82 | 1.86 | |
| | | | | | Mixture 2 | | |
| Methane/74-82-8 | $CH_4$ | 58.31 | 0.09 | Gas Chromatography | 58.56 | 1.17 | Gravimetric method |
| Carbon dioxide/124-38-9 | $CO_2$ | 5.73 | 0.02 | | 5.44 | 0.11 | |
| Hydrogen sulphide/7783-06-4 | $H_2S$ | 35.96 | 0.09 | | 36.00 | 0.72 | |

**Table 2.** Vapour-liquid equilibrium data for Mixture 1. Expanded uncertainties (k=2): U(T) = 0.03 K, U(p) = 0.003 MPa. δx is the repeatability (i.e., the standard deviation of the mean) of the measure.

| p/MPa | T/K | Vapour phase composition (molar fraction) | | | | | | | | |
|---|---|---|---|---|---|---|---|---|---|---|
| | | $CH_4$ | δx | u(x) | $CO_2$ | δx | u(x) | $H_2S$ | δx | u(x) |
| 5.053 | 333.13 | 0.0698 | 0.0006 | 0.0018 | 0.0442 | 0.0005 | 0.0010 | 0.8859 | 0.0009 | 0.0024 |
| 5.419 | 333.14 | 0.1035 | 0.0007 | 0.0025 | 0.0538 | 0.0003 | 0.0012 | 0.8427 | 0.0010 | 0.0032 |
| 5.755 | 333.15 | 0.1335 | 0.0005 | 0.0032 | 0.0588 | 0.0002 | 0.0013 | 0.8077 | 0.0005 | 0.0038 |
| 3.417 | 313.19 | 0.0885 | 0.0003 | 0.0022 | 0.0526 | 0.0003 | 0.0012 | 0.8589 | 0.0005 | 0.0029 |
| 3.870 | 313.19 | 0.1522 | 0.0003 | 0.0035 | 0.0660 | 0.0003 | 0.0014 | 0.7818 | 0.0005 | 0.0042 |
| 4.089 | 313.19 | 0.1802 | 0.0002 | 0.0040 | 0.0689 | 0.0003 | 0.0014 | 0.7509 | 0.0003 | 0.0047 |

| | | | | | | | | | | |
|---|---|---|---|---|---|---|---|---|---|---|
| 2.273 | 293.20 | 0.1312 | 0.0004 | 0.0031 | 0.0677 | 0.0002 | 0.0015 | 0.8011 | 0.0006 | 0.0039 |
| 2.621 | 293.19 | 0.2081 | 0.0004 | 0.0044 | 0.0785 | 0.0003 | 0.0016 | 0.7135 | 0.0006 | 0.0051 |
| 3.009 | 293.23 | 0.2789 | 0.0005 | 0.0054 | 0.0796 | 0.0002 | 0.0016 | 0.6415 | 0.0006 | 0.0059 |
| 1.238 | 273.34 | 0.0953 | 0.0006 | 0.0024 | 0.0595 | 0.0003 | 0.0013 | 0.8452 | 0.0009 | 0.0032 |
| 1.645 | 273.33 | 0.2547 | 0.0004 | 0.0051 | 0.0905 | 0.0002 | 0.0018 | 0.6548 | 0.0005 | 0.0057 |
| 2.023 | 273.35 | 0.3581 | 0.0006 | 0.0061 | 0.0889 | 0.0001 | 0.0017 | 0.5529 | 0.0007 | 0.0064 |
| 1.010 | 253.43 | 0.3405 | 0.0006 | 0.0059 | 0.1027 | 0.0002 | 0.0019 | 0.5568 | 0.0005 | 0.0063 |
| 1.233 | 253.44 | 0.4334 | 0.0008 | 0.0064 | 0.0958 | 0.0006 | 0.0018 | 0.4708 | 0.0008 | 0.0065 |
| 1.420 | 253.42 | 0.493 | 0.001 | 0.0065 | 0.0890 | 0.0006 | 0.0017 | 0.418 | 0.002 | 0.0064 |

1
2

| p/MPa | T/K | Liquid phase composition (molar fraction) | | | | | | | | |
|---|---|---|---|---|---|---|---|---|---|---|
| | | $CH_4$ | δx | u(x) | $CO_2$ | δx | u(x) | $H_2S$ | δx | u(x) |
| 5.053 | 333.13 | 0.0100 | 0.0003 | 0.0003 | 0.0167 | 0.0001 | 0.0004 | 0.9733 | 0.0002 | 0.0006 |
| 5.419 | 333.14 | 0.0158 | 0.0002 | 0.0004 | 0.0218 | 0.0002 | 0.0005 | 0.9624 | 0.0002 | 0.0008 |
| 5.755 | 333.15 | 0.0219 | 0.0002 | 0.0006 | 0.0251 | 0.0003 | 0.0006 | 0.9530 | 0.0002 | 0.0011 |
| 3.417 | 313.19 | 0.0075 | 0.0001 | 0.0002 | 0.0166 | 0.0001 | 0.0004 | 0.9759 | 0.0002 | 0.0005 |
| 3.870 | 313.19 | 0.0151 | 0.0002 | 0.0004 | 0.0234 | 0.0002 | 0.0006 | 0.9615 | 0.0003 | 0.0009 |
| 4.089 | 313.19 | 0.0191 | 0.0001 | 0.0005 | 0.0255 | 0.0002 | 0.0006 | 0.9554 | 0.0002 | 0.0010 |
| 2.273 | 293.20 | 0.0069 | 0.0001 | 0.0002 | 0.0179 | 0.0003 | 0.0004 | 0.9753 | 0.0004 | 0.0006 |
| 2.621 | 293.19 | 0.0129 | 0.0002 | 0.0004 | 0.0238 | 0.0002 | 0.0006 | 0.9633 | 0.0004 | 0.0008 |
| 3.009 | 293.23 | 0.0199 | 0.0002 | 0.0005 | 0.0275 | 0.0003 | 0.0007 | 0.9527 | 0.0003 | 0.0011 |
| 1.238 | 273.34 | 0.0030 | 0.0002 | 0.0001 | 0.0114 | 0.0003 | 0.0003 | 0.9857 | 0.0005 | 0.0003 |
| 1.645 | 273.33 | 0.0095 | 0.0001 | 0.0003 | 0.0238 | 0.0002 | 0.0006 | 0.9667 | 0.0003 | 0.0008 |
| 2.023 | 273.35 | 0.0167 | 0.0001 | 0.0005 | 0.0277 | 0.0001 | 0.0007 | 0.9555 | 0.0002 | 0.0010 |
| 1.010 | 253.43 | 0.0080 | 0.0005 | 0.0002 | 0.0240 | 0.0004 | 0.0006 | 0.9680 | 0.0007 | 0.0007 |
| 1.233 | 253.44 | 0.0117 | 0.0003 | 0.0003 | 0.0272 | 0.0006 | 0.0007 | 0.9612 | 0.0006 | 0.0009 |
| 1.420 | 253.42 | 0.0153 | 0.0002 | 0.0004 | 0.0284 | 0.0002 | 0.0007 | 0.9563 | 0.0002 | 0.0010 |

**Table 3.** Vapour-liquid equilibrium data for Mixture 2. Expanded uncertainties (k=2):U(T) = 0.03 K, U(p) = 0.003 MPa. δx is the repeatability (i.e., the standard deviation of the mean) of the measure.

| p/MPa | T/K | Vapour phase composition (molar fraction) | | | | | | | | |
|---|---|---|---|---|---|---|---|---|---|---|
| | | $CH_4$ | δx | u(x) | $CO_2$ | δx | u(x) | $H_2S$ | δx | u(x) |
| 4.654 | 243.50 | 0.767 | 0.002 | 0.0045 | 0.0553 | 0.0002 | 0.0012 | 0.178 | 0.001 | 0.0040 |
| 9.449 | 243.48 | 0.784 | 0.003 | 0.0043 | 0.0483 | 0.0005 | 0.0010 | 0.168 | 0.003 | 0.0038 |
| 10.244 | 243.50 | 0.711 | 0.001 | 0.0053 | 0.0518 | 0.0005 | 0.0011 | 0.237 | 0.001 | 0.0049 |
| 11.007 | 251.02 | 0.651 | 0.001 | 0.0060 | 0.0553 | 0.0001 | 0.0011 | 0.293 | 0.001 | 0.0056 |
| 4.621 | 253.66 | 0.766 | 0.001 | 0.0045 | 0.0596 | 0.0003 | 0.0013 | 0.174 | 0.001 | 0.0039 |
| 4.608 | 253.65 | 0.766 | 0.002 | 0.0045 | 0.0596 | 0.0004 | 0.0013 | 0.174 | 0.002 | 0.0039 |
| 6.676 | 253.66 | 0.789 | 0.001 | 0.0042 | 0.0552 | 0.0001 | 0.0012 | 0.155 | 0.001 | 0.0036 |
| 8.792 | 253.66 | 0.780 | 0.001 | 0.0044 | 0.0523 | 0.0001 | 0.0011 | 0.167 | 0.001 | 0.0038 |
| 11.198 | 253.49 | 0.639 | 0.001 | 0.0061 | 0.0557 | 0.0001 | 0.0011 | 0.305 | 0.001 | 0.0058 |
| 4.832 | 258.62 | 0.742 | 0.001 | 0.0049 | 0.0597 | 0.0002 | 0.0012 | 0.198 | 0.002 | 0.0043 |
| 9.322 | 258.48 | 0.712 | 0.004 | 0.0053 | 0.0528 | 0.0001 | 0.0011 | 0.236 | 0.004 | 0.0049 |
| 11.236 | 258.48 | 0.667 | 0.002 | 0.0058 | 0.0552 | 0.0001 | 0.0011 | 0.278 | 0.001 | 0.0055 |
| 7.166 | 268.34 | 0.721 | 0.001 | 0.0052 | 0.0585 | 0.0001 | 0.0012 | 0.221 | 0.001 | 0.0047 |
| 8.517 | 268.45 | 0.725 | 0.002 | 0.0051 | 0.057 | 0.0001 | 0.0012 | 0.218 | 0.002 | 0.0047 |
| 7.978 | 278.35 | 0.672 | 0.001 | 0.0057 | 0.0595 | 0.0002 | 0.0012 | 0.269 | 0.001 | 0.0053 |
| 10.567 | 278.32 | 0.654 | 0.001 | 0.0059 | 0.0577 | 0.0002 | 0.0012 | 0.288 | 0.001 | 0.0056 |

| p/MPa | T/K | Liquid phase composition (molar fraction) | | | | | | | | |
|---|---|---|---|---|---|---|---|---|---|---|
| | | $CH_4$ | δx | u(x) | $CO_2$ | δx | u(x) | $H_2S$ | δx | u(x) |
| 4.654 | 243.50 | 0.104 | 0.001 | 0.0025 | 0.0628 | 0.0002 | 0.0014 | 0.833 | 0.001 | 0.0034 |
| 9.449 | 243.48 | 0.331 | 0.005 | 0.0060 | 0.0662 | 0.0002 | 0.0013 | 0.603 | 0.005 | 0.0063 |
| 10.244 | 243.50 | 0.423 | 0.002 | 0.0066 | 0.0617 | 0.0007 | 0.0012 | 0.516 | 0.002 | 0.0067 |
| 11.007 | 251.02 | 0.499 | 0.002 | 0.0067 | 0.0600 | 0.0001 | 0.0012 | 0.441 | 0.002 | 0.0066 |
| 4.621 | 253.66 | 0.0896 | 0.0009 | 0.0022 | 0.0536 | 0.0004 | 0.0012 | 0.857 | 0.001 | 0.0030 |
| 4.608 | 253.65 | 0.090 | 0.001 | 0.0023 | 0.0537 | 0.0002 | 0.0012 | 0.857 | 0.001 | 0.0030 |
| 6.676 | 253.66 | 0.157 | 0.001 | 0.0036 | 0.0645 | 0.0002 | 0.0014 | 0.779 | 0.001 | 0.0043 |
| 8.792 | 253.66 | 0.251 | 0.002 | 0.0051 | 0.0675 | 0.0001 | 0.0014 | 0.681 | 0.002 | 0.0056 |
| 11.198 | 253.49 | 0.514 | 0.002 | 0.0067 | 0.0596 | 0.0001 | 0.0012 | 0.427 | 0.002 | 0.0066 |
| 4.832 | 258.62 | 0.0926 | 0.0006 | 0.0023 | 0.0509 | 0.0001 | 0.0011 | 0.8565 | 0.0006 | 0.0030 |
| 9.322 | 258.48 | 0.271 | 0.003 | 0.0054 | 0.0636 | 0.0003 | 0.0013 | 0.666 | 0.003 | 0.0058 |
| 11.236 | 258.48 | 0.445 | 0.004 | 0.0066 | 0.0614 | 0.0001 | 0.0012 | 0.493 | 0.004 | 0.0067 |
| 7.166 | 268.34 | 0.155 | 0.001 | 0.0036 | 0.0569 | 0.0001 | 0.0012 | 0.788 | 0.001 | 0.0042 |
| 8.517 | 268.45 | 0.211 | 0.002 | 0.0045 | 0.0610 | 0.0001 | 0.0013 | 0.728 | 0.002 | 0.0051 |
| 7.978 | 278.35 | 0.166 | 0.001 | 0.0038 | 0.0540 | 0.0001 | 0.0012 | 0.780 | 0.001 | 0.0043 |
| 10.567 | 278.32 | 0.282 | 0.001 | 0.0055 | 0.0598 | 0.0001 | 0.0012 | 0.659 | 0.001 | 0.0059 |

**Table 4.** Pure compound properties according to the Dortmund Data Bank and the Mathias-Copeman parameters from Reid et al.[41]

| Formula | CAS number | $T_c$/K | $p_c$/MPa | ω | $C_1$ | $C_2$ | $C_3$ |
|---|---|---|---|---|---|---|---|
| $CH_4$ | 74-82-8 | 190.60 | 4.600 | 0.0115 | 0.4157 | -0.1727 | 0.3484 |
| $CO_2$ | 124-38-9 | 304.20 | 7.377 | 0.2236 | 0.7046 | -0.3149 | 1.891 |
| $H_2S$ | 7783-06-4 | 373.55 | 8.937 | 0.1000 | 0.5077 | 0.0076 | 0.3423 |

**Table 5.** Vapor-liquid equilibrium pressures and phase compositions for the $CH_4$ (1)-$CO_2$ (2)-$H_2S$ (3) mixtures. Comparison between the experimental and calculated data determined with the PR EoS and WS mixing rules.

| T/K | $p_{exp}$/MPa | $x_{1\ exp}$ | $x_{2\ exp}$ | $y_{1\ exp}$ | $y_{2\ exp}$ | $y_{3\ exp}$ | $p_{cal}$/MPa | $y_{1\ cal}$ | $y_{2\ cal}$ | $y_{3\ cal}$ |
|---|---|---|---|---|---|---|---|---|---|---|
| 243.50 | 4.654 | 0.104 | 0.0628 | 0.767 | 0.0553 | 0.1777 | 4.533 | 0.8125 | 0.0575 | 0.13 |
| 243.48 | 9.449 | 0.334 | 0.0662 | 0.794 | 0.0483 | 0.1577 | 9.301 | 0.7937 | 0.0483 | 0.158 |
| 243.50 | 10.244 | 0.423 | 0.0617 | 0.711 | 0.0518 | 0.2372 | 10.224 | 0.7353 | 0.0503 | 0.2145 |
| 258.62 | 4.832 | 0.0926 | 0.0509 | 0.742 | 0.0597 | 0.1983 | 4.784 | 0.7384 | 0.0614 | 0.2001 |
| 258.48 | 9.322 | 0.271 | 0.0636 | 0.712 | 0.0528 | 0.2352 | 9.513 | 0.7519 | 0.0537 | 0.1944 |
| 258.48 | 11.236 | 0.445 | 0.0614 | 0.667 | 0.0552 | 0.2778 | 11.683 | 0.6534 | 0.056 | 0.2906 |
| 268.34 | 7.166 | 0.155 | 0.0569 | 0.721 | 0.0585 | 0.2205 | 7.301 | 0.7172 | 0.0603 | 0.2225 |
| 268.45 | 8.517 | 0.211 | 0.061 | 0.725 | 0.057 | 0.218 | 8.837 | 0.7166 | 0.0588 | 0.2246 |
| 253.49 | 11.198 | 0.514 | 0.0596 | 0.639 | 0.0557 | 0.3053 | 11.619 | 0.6162 | 0.0566 | 0.3272 |
| 251.02 | 11.007 | 0.499 | 0.06 | 0.651 | 0.0553 | 0.2937 | 11.355 | 0.6402 | 0.0557 | 0.3042 |
| 253.66 | 4.621 | 0.09 | 0.0536 | 0.766 | 0.0596 | 0.1744 | 4.489 | 0.7595 | 0.0616 | 0.1789 |
| 253.65 | 4.608 | 0.09 | 0.0537 | 0.766 | 0.0596 | 0.1744 | 4.489 | 0.7594 | 0.0617 | 0.1789 |
| 253.66 | 6.676 | 0.157 | 0.0645 | 0.789 | 0.0552 | 0.1558 | 6.578 | 0.7853 | 0.0573 | 0.1574 |
| 253.66 | 8.792 | 0.251 | 0.0675 | 0.78 | 0.0523 | 0.1677 | 8.766 | 0.778 | 0.054 | 0.1679 |
| 278.35 | 7.978 | 0.166 | 0.054 | 0.672 | 0.0595 | 0.2685 | 8.154 | 0.6663 | 0.061 | 0.2727 |
| 278.32 | 10.567 | 0.282 | 0.0598 | 0.654 | 0.0577 | 0.2883 | 10.965 | 0.6449 | 0.0592 | 0.2959 |
| 333.13 | 5.053 | 0.01 | 0.0167 | 0.0698 | 0.0442 | 0.886 | 5.06 | 0.0656 | 0.0418 | 0.8927 |
| 333.14 | 5.419 | 0.0158 | 0.0218 | 0.1035 | 0.0538 | 0.8427 | 5.401 | 0.0948 | 0.0512 | 0.854 |
| 333.15 | 5.755 | 0.0219 | 0.0251 | 0.1335 | 0.0588 | 0.8077 | 5.726 | 0.1215 | 0.0558 | 0.8227 |
| 313.19 | 3.417 | 0.0075 | 0.0166 | 0.0885 | 0.0526 | 0.8589 | 3.43 | 0.0868 | 0.0529 | 0.8603 |
| 313.19 | 3.870 | 0.0151 | 0.0234 | 0.1522 | 0.066 | 0.7818 | 3.884 | 0.1507 | 0.0663 | 0.7829 |
| 313.19 | 4.089 | 0.0191 | 0.0255 | 0.1802 | 0.0689 | 0.7509 | 4.102 | 0.1787 | 0.0688 | 0.7525 |
| 293.20 | 2.273 | 0.0069 | 0.0179 | 0.1312 | 0.0677 | 0.8011 | 2.292 | 0.1318 | 0.0682 | 0.7999 |
| 293.19 | 2.621 | 0.0129 | 0.0238 | 0.2081 | 0.0785 | 0.7134 | 2.645 | 0.2101 | 0.0792 | 0.7107 |
| 293.23 | 3.009 | 0.0199 | 0.0275 | 0.2789 | 0.0796 | 0.6415 | 3.025 | 0.2792 | 0.0809 | 0.6399 |
| 273.34 | 1.238 | 0.003 | 0.0114 | 0.0953 | 0.0595 | 0.8452 | 1.263 | 0.1105 | 0.0588 | 0.8307 |
| 273.33 | 1.645 | 0.0095 | 0.0238 | 0.2547 | 0.0905 | 0.6548 | 1.664 | 0.2586 | 0.093 | 0.6483 |
| 273.35 | 2.023 | 0.0167 | 0.0277 | 0.3581 | 0.0889 | 0.553 | 2.042 | 0.3652 | 0.0894 | 0.5453 |
| 253.43 | 1.010 | 0.008 | 0.024 | 0.3405 | 0.1027 | 0.5568 | 1.038 | 0.3493 | 0.1026 | 0.5481 |

| | | | | | | | | | | |
|---|---|---|---|---|---|---|---|---|---|---|
| 253.44 | 1.233 | 0.0117 | 0.0272 | 0.4334 | 0.0958 | 0.4708 | 1.225 | 0.4286 | 0.099 | 0.4724 |
| 253.42 | 1.420 | 0.0153 | 0.0284 | 0.493 | 0.089 | 0.418 | 1.398 | 0.4881 | 0.0913 | 0.4206 |

**Table 6a.** Values of the NRTL binary interaction parameters.

| $\tau_{ij}$/J.mol$^{-1}$ | $CH_4$ | $CO_2$ | $H_2S$ |
|---|---|---|---|
| $CH_4$ | - | 89 | 1119 |
| $CO_2$ | 3117 | - | 1140 |
| $H_2S$ | 2504 | 1904 | - |

**Table 6b.** Values of the $k_{ij}$ binary interaction parameters.

| $k_{12}$ | $CH_4$ | $CO_2$ | $H_2S$ |
|---|---|---|---|
| $CH_4$ | - | 0.20266 | 0.22719 |
| $CO_2$ | 0.20266 | - | 0.04398 |
| $H_2S$ | 0.22719 | 0.04398 | - |

**Table 7.** Vapor-liquid equilibrium pressures and phase compositions for the $CH_4$ (1)-$CO_2$ (2)-$H_2S$ (3) mixture (data from Ng et al.). Comparison between the experimental and calculated data determined with the PR EoS and WS mixing rules.

| T/K | $p_{exp}$/MPa | $x_{1\ exp}$ | $x_{2\ exp}$ | $y_{1\ exp}$ | $y_{2\ exp}$ | $p_{cal}$/MPa | $y_{1\ cal}$ | $y_{2\ cal}$ |
|---|---|---|---|---|---|---|---|---|
| 199.15 | 1.499 | 0.0431 | 0.1313 | 0.9002 | 0.0648 | 1.2418 | 0.8881 | 0.0693 |
| 199.15 | 2.865 | 0.0971 | 0.1488 | 0.9317 | 0.0430 | 2.2399 | 0.9263 | 0.0459 |
| 199.15 | 4.195 | 0.1893 | 0.1424 | 0.9410 | 0.0338 | 3.3499 | 0.9428 | 0.0336 |
| 199.15 | 0.925 | 0.0357 | 0.3879 | 0.8015 | 0.1584 | 0.8838 | 0.7874 | 0.1648 |
| 199.15 | 2.838 | 0.1515 | 0.3129 | 0.9144 | 0.0628 | 2.4423 | 0.9118 | 0.0649 |
| 199.48 | 2.388 | 0.1314 | 0.4128 | 0.8761 | 0.0901 | 2.1325 | 0.8932 | 0.0832 |
| 199.54 | 3.519 | 0.2691 | 0.3652 | 0.8980 | 0.0700 | 3.0566 | 0.9168 | 0.0638 |
| 199.65 | 4.145 | 0.4283 | 0.2482 | 0.9260 | 0.0508 | 3.7214 | 0.9312 | 0.0483 |
| 204.65 | 2.703 | 0.1531 | 0.6609 | 0.8620 | 0.1228 | 2.5016 | 0.8590 | 0.1244 |
| 204.85 | 3.965 | 0.3301 | 0.5411 | 0.8885 | 0.0992 | 3.5680 | 0.8857 | 0.1019 |
| 206.15 | 1.378 | 0.0576 | 0.7156 | 0.7554 | 0.2126 | 1.3937 | 0.7628 | 0.2078 |
| 215.65 | 2.511 | 0.0734 | 0.1756 | 0.8515 | 0.0941 | 2.2607 | 0.8438 | 0.0956 |
| 215.65 | 4.573 | 0.2100 | 0.2453 | 0.8774 | 0.0810 | 4.0491 | 0.8782 | 0.0789 |
| 216.15 | 6.142 | 0.6272 | 0.1639 | 0.8732 | 0.0745 | 5.9673 | 0.8834 | 0.0693 |
| 226.76 | 5.668 | 0.3140 | 0.3217 | 0.8141 | 0.1258 | 5.3697 | 0.8223 | 0.1223 |
| 226.87 | 4.109 | 0.1677 | 0.3692 | 0.7817 | 0.1515 | 3.8890 | 0.7926 | 0.1479 |
| 226.95 | 5.506 | 0.3336 | 0.5327 | 0.7824 | 0.1880 | 5.2972 | 0.7824 | 0.1895 |
| 227.15 | 1.731 | 0.0408 | 0.2841 | 0.6593 | 0.2353 | 1.6771 | 0.6468 | 0.2390 |
| 227.45 | 7.777 | 0.2941 | 0.1020 | 0.8218 | 0.0645 | 6.7682 | 0.8694 | 0.0505 |
| 227.55 | 2.827 | 0.0626 | 0.1080 | 0.8226 | 0.0867 | 2.5006 | 0.8099 | 0.0918 |
| 227.55 | 4.864 | 0.1404 | 0.1273 | 0.8622 | 0.0674 | 4.3530 | 0.8572 | 0.0698 |
| 232.98 | 4.486 | 0.1346 | 0.1619 | 0.8165 | 0.0978 | 4.3312 | 0.8176 | 0.0962 |
| 233.04 | 5.852 | 0.2147 | 0.1902 | 0.8237 | 0.0968 | 5.5287 | 0.8243 | 0.0953 |
| 233.15 | 6.950 | 0.3095 | 0.1940 | 0.8135 | 0.0982 | 6.5007 | 0.8233 | 0.0940 |
| 254.85 | 6.171 | 0.1864 | 0.3198 | 0.6506 | 0.2163 | 6.0146 | 0.6521 | 0.2149 |
| 254.95 | 6.812 | 0.1641 | 0.1076 | 0.7563 | 0.0882 | 6.4674 | 0.7527 | 0.0901 |
| 254.95 | 9.060 | 0.2583 | 0.1076 | 0.7412 | 0.0847 | 8.4115 | 0.7532 | 0.0822 |

| | | | | | | | | |
|---|---|---|---|---|---|---|---|---|
| 254.95 | 5.528 | 0.1687 | 0.6229 | 0.5472 | 0.3754 | 5.5495 | 0.5490 | 0.3750 |
| 255.05 | 6.895 | 0.2639 | 0.5708 | 0.5785 | 0.3505 | 6.9030 | 0.5797 | 0.3512 |
| 255.05 | 8.122 | 0.3784 | 0.4930 | 0.5699 | 0.3553 | 8.0494 | 0.5768 | 0.3513 |
| 255.15 | 3.513 | 0.0569 | 0.0769 | 0.6808 | 0.1071 | 3.2378 | 0.6699 | 0.1100 |
| 255.15 | 3.524 | 0.0645 | 0.2388 | 0.5622 | 0.2505 | 3.4060 | 0.5593 | 0.2516 |
| 255.15 | 8.501 | 0.3637 | 0.2939 | 0.6539 | 0.2054 | 8.2855 | 0.6574 | 0.2027 |
| 277.15 | 7.681 | 0.1792 | 0.2746 | 0.5213 | 0.2499 | 7.5311 | 0.5212 | 0.2480 |
| 277.25 | 9.515 | 0.2764 | 0.2861 | 0.5156 | 0.2503 | 9.1125 | 0.5155 | 0.2486 |
| 282.15 | 5.948 | 0.0885 | 0.0827 | 0.5804 | 0.1034 | 5.5900 | 0.5588 | 0.1187 |
| 282.65 | 10.549 | 0.2677 | 0.0985 | 0.5959 | 0.0958 | 10.4510 | 0.5984 | 0.0976 |
| 283.15 | 8.239 | 0.1632 | 0.0897 | 0.6102 | 0.0996 | 8.0840 | 0.6065 | 0.1013 |
| 285.40 | 11.838 | 0.3585 | 0.0983 | 0.5066 | 0.0980 | 11.8980 | 0.5376 | 0.0969 |

1

2

**Table 8.** Group interaction parameters[3,43,44] ($A_{kl} = A_{lk}$)/MPa and ($B_{kl} = B_{lk}$)/MPa needed to apply the PPR78 model.

| | $CH_4$ (group 5) | $CO_2$ (group 12) | $H_2S$ (group 14) |
|---|---|---|---|
| $CH_4$ (group 5) | 0 | | |
| $CO_2$ (group 12) | $A_{12\text{-}5} = 136.57$<br>$B_{12\text{-}5} = 214.81$ | 0 | |
| $H_2S$ (group 14) | $A_{14\text{-}5} = 190.10$<br>$B_{14\text{-}5} = 307.46$ | $A_{14\text{-}12} = 135.20$<br>$B_{14\text{-}12} = 199.02$ | 0 |

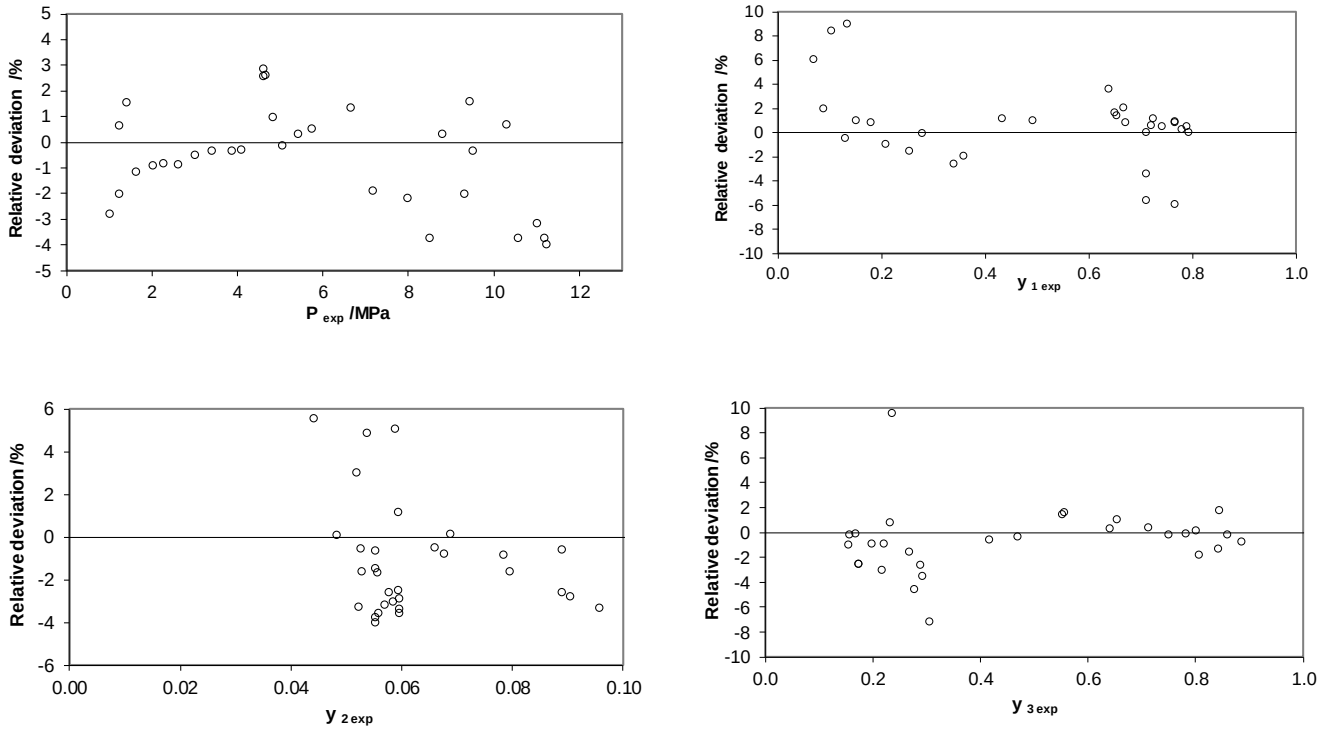


1 **Figure 1.** Relative deviations between the calculated (with the PR EoS and WS mixing rules) and
2 experimental bubble pressure and vapour phase composition. These data were measured in this
3 study.
4

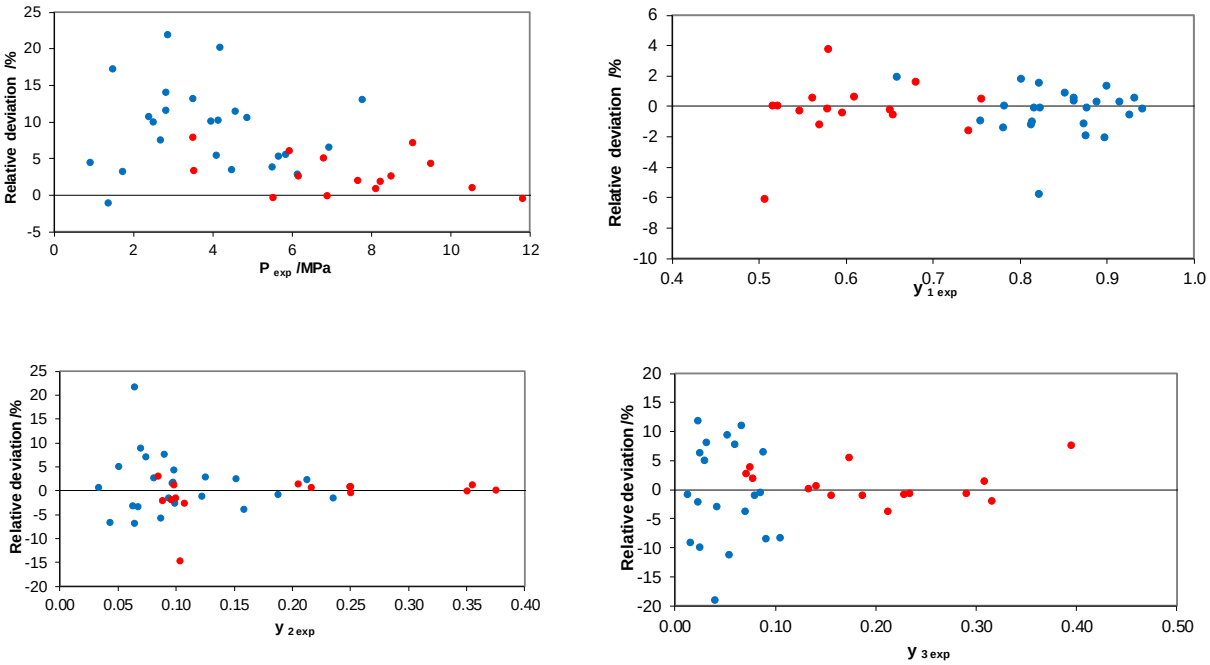


**Figure 2.** Relative deviations between the calculated (with the PR EoS and WS mixing rules) and experimental bubble pressure and vapour phase composition. The data were obtained from Ng et al., and the model parameters were adjusted based on the data acquired in this work (● 199 < T/K < 234, ● 254 < T/K < 286).

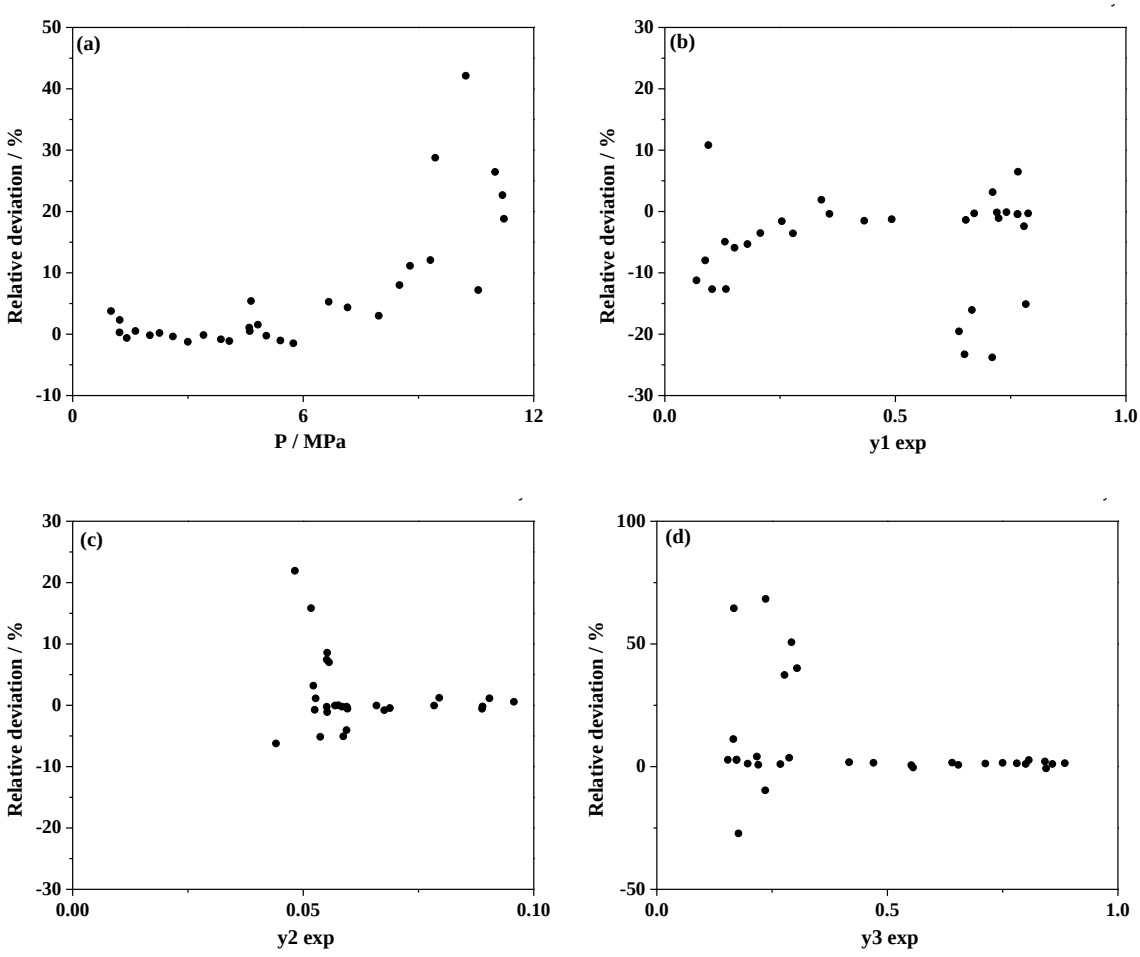


**Figure 3.** Relative deviations between the calculated (with the PPR78 model) and experimental bubble pressure (a) and vapour phase composition (b-d) measured in this study.

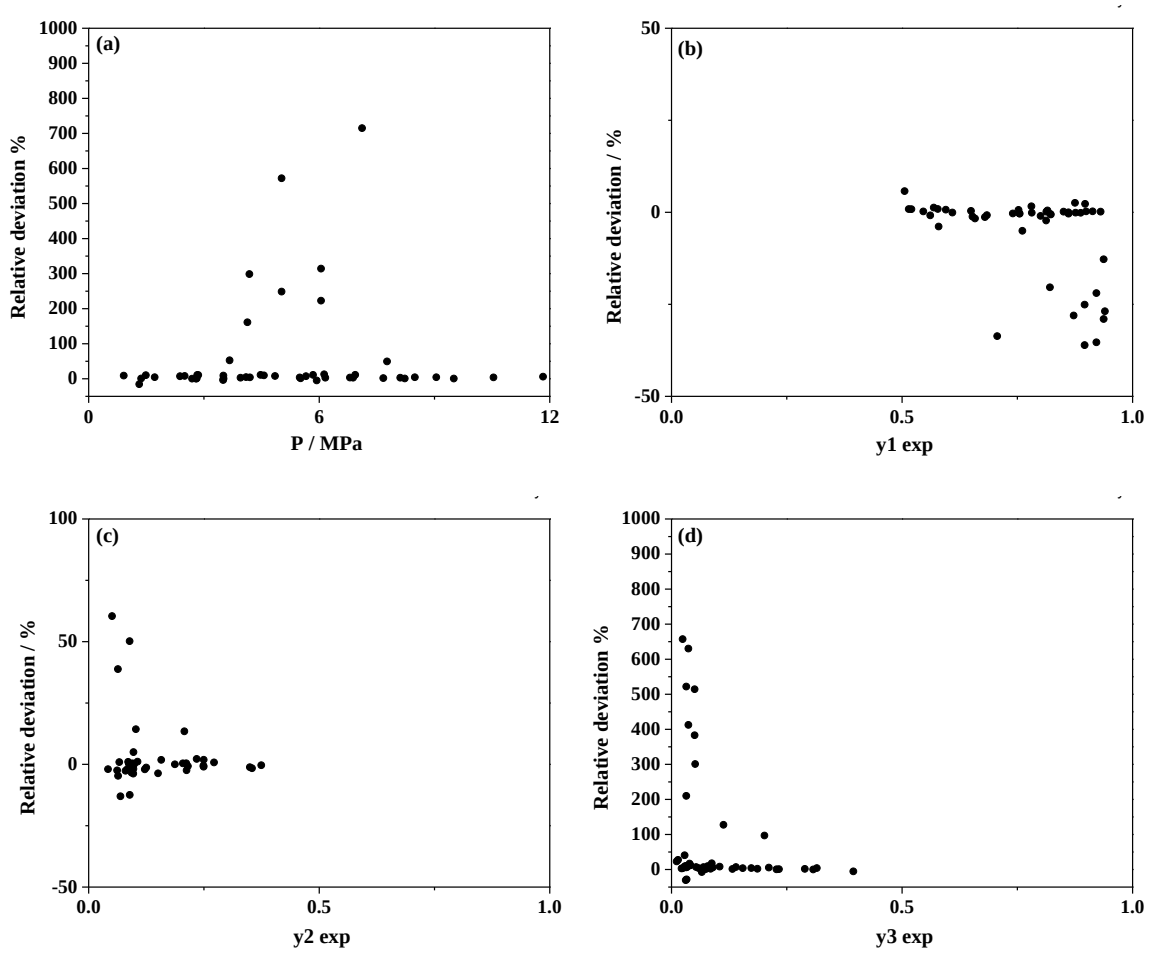


**Figure 4.** Relative deviations between the calculated (with the PPR78 model) and experimental bubble pressure (a) and vapour phase composition (b-d). The data were obtained from Ng et al.

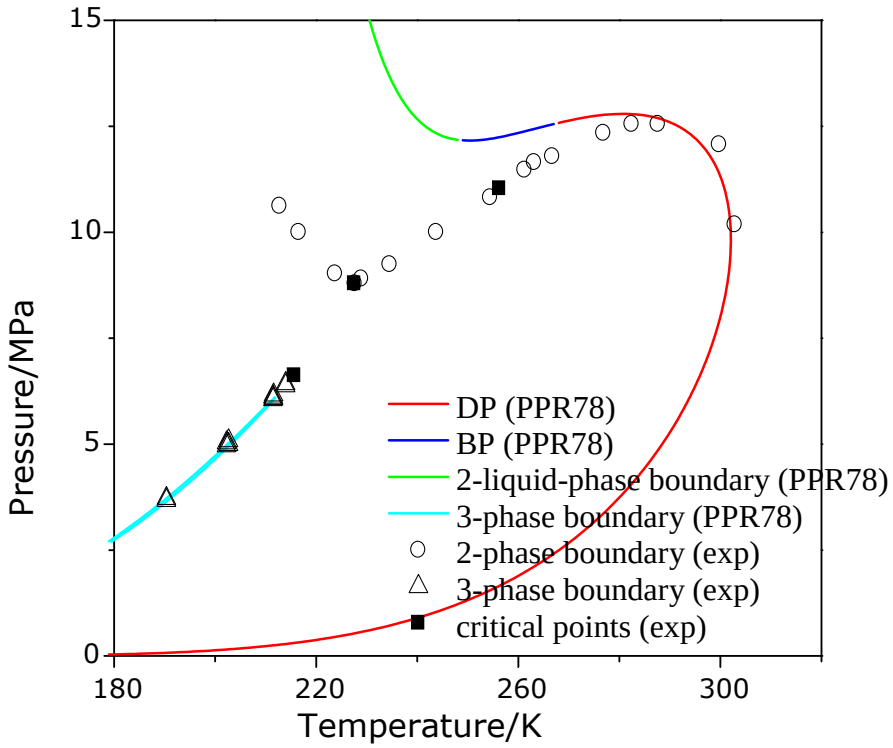


**Figure 5.** PT phase envelope of the $CH_4$ (1) + $CO_2$ (2) + $H_2S$ (3) mixture ($x_1$ = 0.4988, $x_2$ = 0.0987, $x_3$ = 0.4022) as predicted by the PPR78 model. The experimental data (according to the symbols) are those reported by Ng et al. DP = dew-point curve, BP = bubble-point curve.

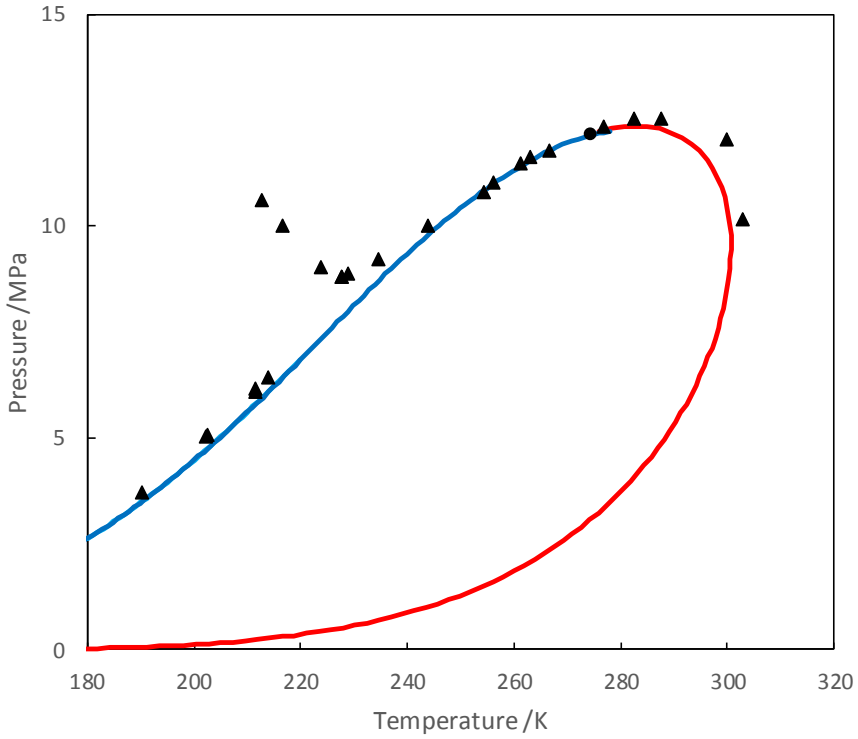


**Figure 6.** PT phase envelope of the $CH_4$ (1) + $CO_2$ (2) + $H_2S$ (3) mixture ($x_1$ = 0.4988, $x_2$ = 0.0987, $x_3$ = 0.4022) as predicted with the PR EoS and WS mixing rules. The experimental data (according to the symbols) are those reported by Ng et al.

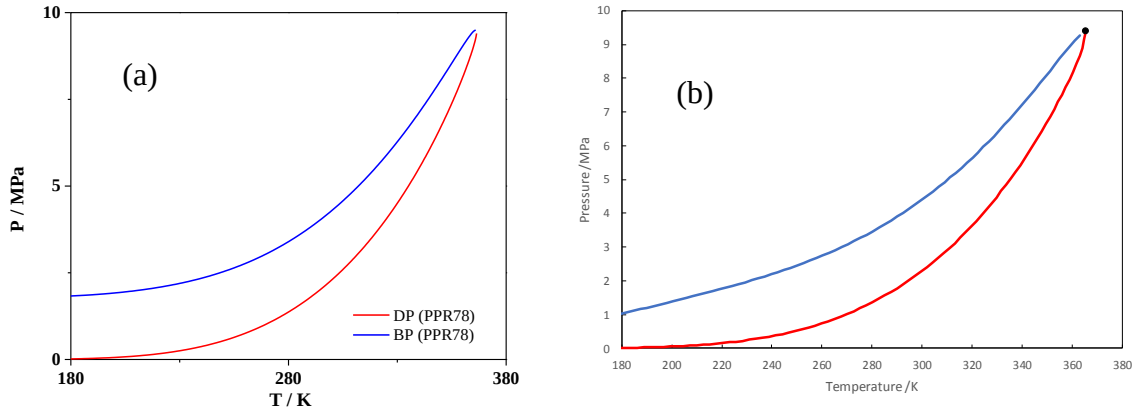


**Figure 7.** PT phase envelope of $CH_4$ (1) + $CO_2$ (2) + $H_2S$ (3) mixture 1 ($x_1$ = 0.0406, $x_2$ = 0.0311, $x_3$ = 0.9283) studied in this work. (a) Prediction with the PPR78 model. (b) Prediction with the PR EoS and WS mixing rules (symbol: calculated critical point). DP = dew-point curve, BP = bubble-point curve.

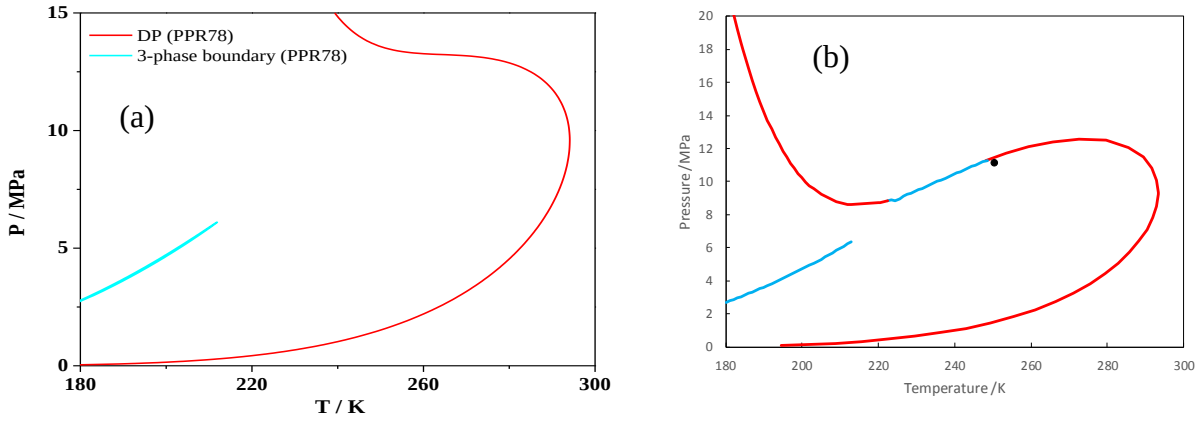


**Figure 8.** PT phase envelope of $CH_4$ (1) + $CO_2$ (2) + $H_2S$ (3) mixture 2 ($x_1$ = 0.5831, $x_2$ = 0.0573, $x_3$ = 0.3596) studied in this work. (a) Prediction with the PPR78 model. (b) Prediction with the PR EoS and WS mixing rules (symbol: calculated critical point). DP = dew-point curve.

**TOC Graphic**

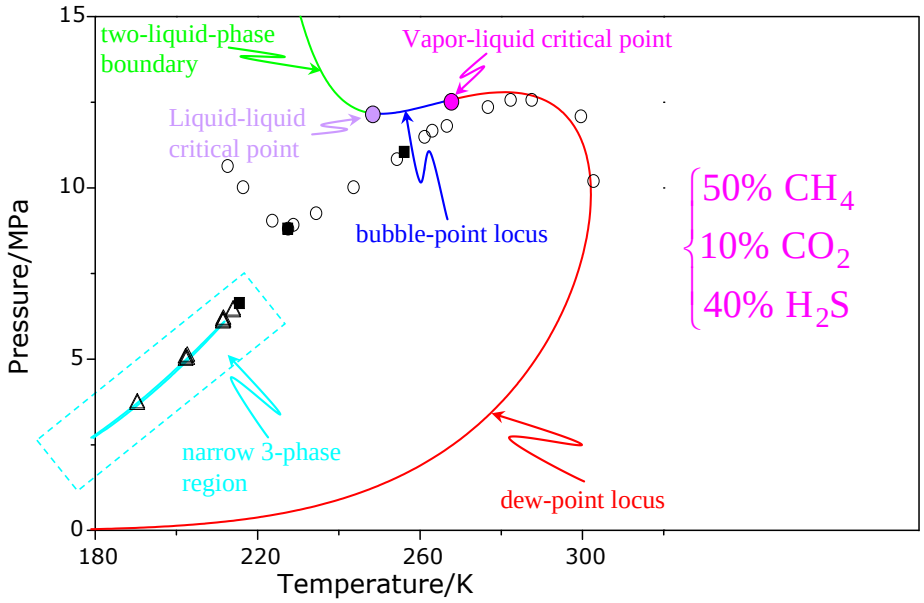
two-liquid-phase boundary
Vapor-liquid critical point
Liquid-liquid critical point
bubble-point locus
50% $CH_4$
10% $CO_2$
40% $H_2S$
narrow 3-phase region
dew-point locus
Pressure/MPa
Temperature/K
15
10
5
0
180
220
260
300